Functionalized Multi Walled Carbon Nanotubes Nano Biocomposite Film for the Amperometric Detection of L-Cysteine

Soundappan Thiagarajan, Yogeswaran Umasankar, and Shen-Ming Chen*

Electroanalysis and Bioelectrochemistry Lab, Department of Chemical Engineering and Biotechnology, National Taipei University of Technology, No. 1, Section 3, Taipei 106, Taiwan, Republic of China

The development of nano biocomposite film (*f*-MWCNTs-Au-GO*x*) for L-cysteine (LC) detection is proposed by using glassy carbon electrode (GCE). The proposed nano biocomposite film has been fabricated on ITO for scanning electron microscopy (SEM) and atomic force microscopy (AFM) analysis. Next, the *f*-MWCNTs-Au-GO*x* nano biocomposite film modified GCE's surface was examined by scanning electrochemical microscopy (SECM). The proposed nano biocomposite film has been successfully applied for the detection of LC using cyclic voltammetry (CV) and amperometry. The *f*-MWCNTs-Au-GO*x* film modified GCE exhibited a linear response for LC detection in the lower and higher concentrations ranges of 2 to 42×10^{-6}, 0.1 to 1.08×10^{-3} mol L^{-1}. Also, the proposed nano biocomposite film possesses high sensitivity and good repeatability for LC detection.

Keywords: Functionalized Multi-Walled Carbon Nanotubes, Gold Nanoparticles, Glucose Oxidase, L-Cysteine, Amperometry.

1. INTRODUCTION

Cysteine is a α-amino acid and denoted as a non-essential amino acid in human metabolism. Although classified as a non-essential amino acid, in rare cases, cysteine may be essential for infants, the elderly, and individuals with certain metabolic disease or who suffer from malabsorption syndromes. Further it is also used in medicine and food industries. Thus, the development of sensitive and accurate determination method for the cysteine oxidation is essential in analytical chemistry. Utilizing the electrochemical techniques for the detection and determination of cysteine appears to be best among the other favorites, because the electrochemical detection provide interesting results for cysteine. For example, L-cysteine has been studied widely on bare electrode materials like mercury,[1–2] platinum,[3,4] gold[5] and carbon.[6] However, the direct oxidations of cysteine, at these solid electrodes were kinetically slow and require a large over potentials.

On the other hand, film modified electrodes have been found as to be interesting and efficient for the detection of cysteine. For example, porphyrins,[7] multilayer films,[8] fullerene,[9] cytochrome C on a DNA,[10] cobalt, manganese and zinc phthalocyanine complexes,[11] ruthenium oxide/hexacyanoferrate and ruthenium hexacyanoferrate mixed films,[12] multi-vanadium-substituted polyoxometalates,[13] poly(nickel tetrakis (*N*-methyl-4-pyridyl)porphyrin) tetratosylate,[14] mixed-valent of ruthenium oxide/hexacyanoferrate/silicomolybdate hybrid films modified glassy carbon electrode (GCE) have been reported.[15] Next, cobalt tetra-aminophthalocyanine film modified vitreous carbon electrode,[16] functionalized multi-wall carbon nanotubes modified electrode,[17] coenzyme B$_{12}$ modified graphite electrode,[18] ferrocenecarboxylic acid modified carbon paste electrode,[19] self-assembled monolayers (SAMs) on gold electrodes,[20] ferrocene dicarboxylic acid modified carbon paste electrode,[21] carbon ionic liquid electrode,[22] erbium hexacyanoferrate-modified carbon ceramic electrode,[23] inorganic–organic complex with a vanadium-substituted polyoxometalate modified carbon paste electrode[24] have been reported for the cysteine detection process. Among these electrode substrates, CNTs show interesting electrocatalytic activities for the cysteine oxidation.[17]

Further the immobilization of proteins on nanostructured materials such as colloidal gold, montmorillonite, clay, mesoporous materials and molecular sieves have been identified as very promising methods for biosensing applications.[25–28] Generally, the chemical functionalization of the enzyme layer with tethered redox-relay groups is

---

helpful for the establishment of unprecedented efficient electron-transfer communication between redox proteins and electrodes.[29] These integrated enzyme electrodes were prepared by the cross-linking of layered affinity complexes between cofactor and the enzyme.[30] Several techniques have been tailored for the use of Au with enzymes, which includes the reconstituted apo-glucose oxidase (apo-GO*x*) on pyrroloquinoline quinone (PQQ)-flavin adenine dinucleotide (FAD). In another method, apo-GO*x* on FAD-functionalized Au linked to the gold electrode surface by a dithiol monolayer.[31] Further, based on the above literature reports it concludes that the combination of functionalized multi wall carbon nanotubes combined with gold nanoparticles and glucose oxidase enzyme will possess the excellent electrocatalytic properties for the biomolecules.

Herein, we report the enzyme biocomposite film (*f*-MWCNTs-Au-GO*x*) using functionalized multiwall carbon nanotubes (*f*-MWCNTs) with nano gold (Au) and glucose oxidase (GO*x*). The film formation process involves the modification of GCE with uniformly well dispersed *f*-MWCNTs aqueous solution, and then it has been electrochemically deposited from an aqueous solution following with the uniform thin layer coating of GO*x*. The morphology of the film has been studied using scanning electron microscopy (SEM), atomic force microscopy (AFM) and scanning electrochemical microscopy (SECM). The SECM technique has shown great promise for the studies of immobilized bio molecules with chemical, biological reactions at the electrode solution interface.[32, 33] Initially, our studies show that SECM is suitable for imaging *f*-MWCNTs-Au-GO*x*, because its imaging parameters are compatible. In addition, the SECM topographic imaging of *f*-MWCNTs-Au-GO*x* has been done through the oxidation of potassium hexacyanoferrate. Further the proposed nano biocomposite film successfully applied for the electrocatalytic oxidation of LC using CV and amperometry. Finally, the proposed *f*-MWCNTs-Au-GO*x* biocomposite enzyme GCE has been used as an amperometric sensor for the detection of LC in wide concentration ranges, respectively.

2. EXPERIMENTAL DETAILS

2.1. Reagents

$KAuCl_4 \cdot 3H_2O$, glucose oxidase, multiwall carbon nanotubes (MWCNTs OD = 10–20 nm, ID = 2–10 nm and length = 0.5–200 μm), LC obtained from Sigma-Aldrich (USA) was used as received. All other chemicals used were of analytical grade. The preparations of aqueous solutions were done with twice distilled deionized water. Solutions were deoxygenated by purging with pre-purified nitrogen gas. Buffer solutions were prepared from 0.5 mol L^{-1} H_2SO_4 and phosphate buffer (0.1 mol L^{-1} NaH_2PO_4 and 0.1 mol $L^{-1} NaH_2PO_4$) (PBS) for the pH 7.4 aqueous solutions.

2.2. Apparatus

Cyclic voltammetry (CV) and amperometric *i–t* curve were performed in an analytical system model CHI-400 and CHI-750 potentiostat (CH Instruments Inc., USA) respectively. A conventional three-electrode cell assembly consisting of an Ag/AgCl reference electrode and a Pt wire counter electrode were used for the electrochemical measurements. The working electrode was either an unmodified GCE (area = 0.07 cm^2) or a GCE modified with the nano biocomposite films and all the potentials have been reported versus the Ag/AgCl reference electrode. The disposable screen-printed carbon electrode (SPCE) with a radius of 5 mm was purchased from Zensor R&D (Taichung, Taiwan). The morphological characterizations of the film were examined by means of SEM (Hitachi S-3000H, Japan) and AFM (Being Nano-Instruments CSPM 4000, China). A SECM model 900 (CH Instruments Inc., USA) was used to control the tip potentials for measuring the topographic current image of the biocomposite film. A Pt ultramicroelectrode (UME) of 7 μm diameter was employed as an SECM tip. The auxiliary and reference electrode for the SECM measurement was a Pt wire and an Ag/AgCl (1 mol L^{-1} KCl) electrode. All the electrochemical measurements were carried out at 25 °C $\pm$ 2.

2.3. Fabrication of *f*-MWCNTs-Au-GO*x* Biocomposite Electrode

Important challenge in the preparation of *f*-MWCNTs is the difficulty in dispersing it into a homogeneous solution. Based on the previous literature report,[34] the functionalization of MWCNTs were done by weighing 10 mg of MWCNTs and 200 mg of potassium hydroxide in to a ruby mortar and grounded together for 2 h at room temperature (28 °C $\pm$ 2). Then, the reaction mixture was dissolved in 10 ml of double distilled deionized water, and then precipitated many times into methanol for the complete removal of potassium hydroxide. The obtained *f*-MWCNTs in water were ultra sonicated for 6 hour to get a uniform dispersion. The functionalization of MWCNTs was obtained by the complete homogeneous dispersion in water.[34] A homogenous GO*x* solution was prepared by dissolving 5 mg of GO*x* in 1 ml of double distilled deionized water. Before starting each experiment, the GCEs were polished by a BAS polishing kit with 0.05 μm alumina slurry, rinsed and then ultrasonicated in double distilled deionized water. The GCE was uniformly coated with 6 μl of *f*-MWCNTs and dried at about 40 °C. Then, the Au has been electrodeposited on the *f*-MWCNTs modified GCE by immersing it in 0.5 mol L^{-1} H_2SO_4 aqueous solution containing $KAuCl_4 \cdot 3H_2O$ (2×10^{-3} mol L^{-1}). Here the electrochemical deposition process of Au has been carried by using consecutive CV in a suitable potential range of 1.1 to 0 V for fifteen cycles

(charge involved $= 3.102 \times 10^{-5}$ C). Further, the modified *f*-MWCNTs-Au electrode was carefully washed with double distilled deionized water to remove the H_2SO_4 and then a thin layer of 2 μL GO*x* has been coated and dried at the room temperature.
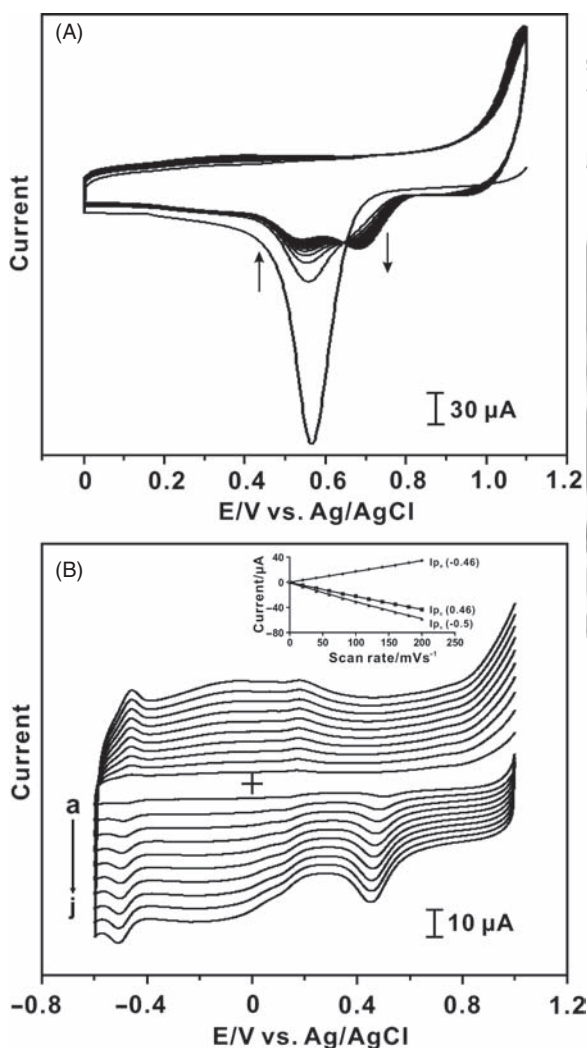
3. RESULTS AND DISCUSSION

3.1. Electrochemical Properties of *f*-MWCNTs-Au-GO*x* Film

Figure 1(A) shows the electrochemical deposition of Au on the *f*-MWCNTs modified GCE. At initial, the reduction of Au begins around 0.53 V and decreases for the continuous cycling and ends around 0.52 V. This happens

Fig. 1. (A) Repetitive CVs of Au deposition process on *f*-MWCNTs modified GCE from 0.5 mol L^{-1} H_2SO_4 aqueous solution containing 2×10^{-3} mol L^{-1} $KAuCl_4 \cdot 3H_2O$ at the scan rate of 100 mV s^{-1}. (B) CVs of the *f*-MWCNTs-Au-GO*x* biocomposite in pH 7.4 PBS: scan rate (a) 20 to (j) 200 mV s^{-1}. The inset in (B) shows a plot of peak currents Ip_a (−0.46) and Ip_c (0.46 and −0.5) versus scan rate.
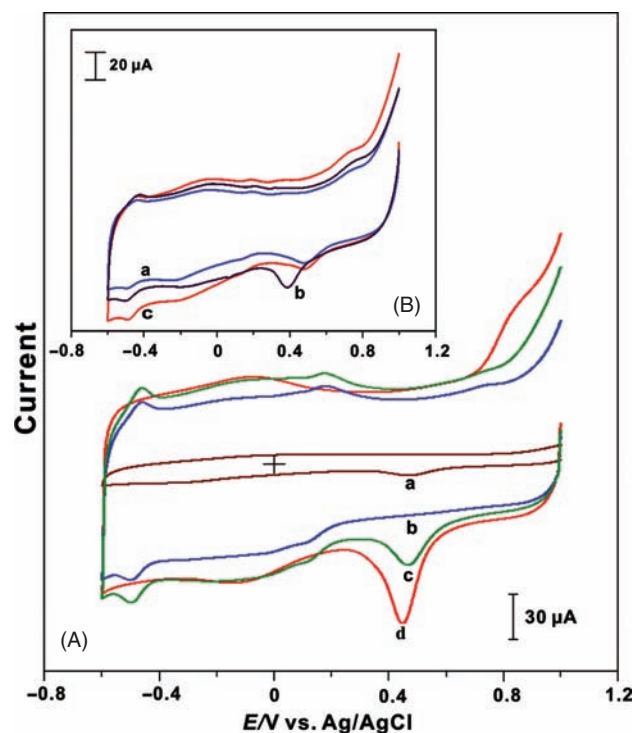
because the presence of *f*-MWCNTs modified GCE surface which alters the reduction peak of Au from 0.52 to 0.67 V. Further for continuous cycling process, the reduction and oxidation peaks of Au are found growing at 0.67 and 1.05 V which indicates the electro deposition of Au on the *f*-MWCNTs modified GCE, respectively. After the GO*x* modification, the nanocomposite film modified GCE has been transferred to pH 7.4 PBS for the different scan rate studies. Figure 1(B) shows different scan rate study of the *f*-MWCNTs-Au-GO*x* film modified GCE in pH 7.4 PBS (up to 200 mV s^{-1}). Here, the *f*-MWCNTs-Au-GO*x* biocomposite enzyme film modified GCE exhibits three redox couples at $E^{o\prime} = 0.14$ V, -0.48 V, -0.15 V and one $Ep_c = 0.45$ V, which corresponds to the electrochemical response of GO*x*, FAD, *f*-MWCNTs, and nano Au respectively. From these different scan rate studies, it shows that the anodic and cathodic peak currents of the nano biocomposite film increase linearly with the increasing scan rate up to 200 mV s^{-1}, which confirms that the film is electrochemically active and stable in pH 7.4. Further the inset in Figure 1(B) shows the Ip versus scan rate plot for the cathodic and anodic peaks at 0.46, -0.46, and -0.5 and were found as linear up to 200 mV s^{-1}.

To elucidate the importance of the proposed film, various type of films such like Au-GO*x*, *f*-MWCNTs-GO*x*, *f*-MWCNTs-Au-GO*x* and *f*-MWCNTs-Au (Fig. 2(A)) have been prepared and studied using CV in pH 7.4 PBS for the detailed comparison studies. Here the CV curve in Figure 2(A) (a) shows the Au-GO*x* film with two reduction peak potentials at $Ep_c = 0.45$ V and -0.33 V represents nano Au and GO*x*. Comparing the Figure 2(A) (a) curve with Figure 2(A) (b) (*f*-MWCNTs-GO*x*), it shows that the activity of GO*x* and its co-enzyme (FAD) is lower in the presence of Au than at *f*-MWCNTs (supporting evidence has been discussed in the upcoming LC electro catalysis section). Further the formal potential of GO*x* and FAD in curve (b) is found as $E^{o\prime} = 0.14$ and -0.48 V, and a broad peak appeared at $E^{o\prime} = -0.15$ V confirms the presence of *f*-MWCNTs, respectively.

The Figure 2(A) curve (c) (*f*-MWCNTs-Au-GO*x* biocomposite enzyme film) shows three redox couples at $E^{o\prime} = 0.14$ V, -0.48 V, -0.15 V and one $Ep_c = 0.45$ V, which represents the redox reactions of GO*x*, FAD, *f*-MWCNTs, and nano Au, respectively. Further Figure 2(A) curve (d) shows the absence of GO*x* on the *f*-MWCNTs-Au composite film, possess higher peak current $Ip_c = 35.5$ μA for Au comparing with all other type of film modified GCEs; *f*-MWCNTs-Au-GO*x* ($Ip_c = 22.4$ μA) and Au-GO*x* ($Ip_c = 2.6$ μA). From the above results, the activity of *f*-MWCNTs could be explained by comparing curve (a) to (c) and (d), where the magnitude of the peak current and the films' current increases in the presence of *f*-MWCNTs, respectively. This occurs because the capacitive current nature of *f*-MWCNTs, respectively. Further the activity of Au present in the biocomposite film could

Fig. 2. (A) CVs of (a) Au-GO*x*, (b) *f*-MWCNTs-GO*x*, (c) *f*-MWCNTs-Au-GO*x* biocomposite enzyme film and (d) *f*-MWCNTs-Au in pH 7.4 PBS: scan rate 100 mV s⁻¹. (B) show the cyclic voltammograms of MWCNTs-Au-GO*x* biocomposite enzyme film at (pH 7.4 PBS) (a) screen printed carbon electrode (SPCE), (b) gold electrode and (c) GCE.

be explained by comparing curve (b) with (c), and there is an increase in the peak current and which was found in curve (c). These results prove that the *f*-MWCNTs and Au enhances the activity and the current magnitude of *f*-MWCNTs-Au-GO*x* film. Also, the presence of *f*-MWCNTs supports the catalytic activity of GO*x* and FAD, respectively.

Further three different type of electrodes GCE, gold electrode (GE) and screen printed carbon electrode (SPCE) (Fig. 2(B)) were used to study the nature of nano biocomposite film. Here except GE (Fig. 2(B) curve (b)), the remaining two electrodes (GCE and SPCE Fig. 2(B) curve (c) and curve (a)) exhibits the Au reduction, FAD and GO*x* redox couples at almost similar potentials. Especially, in GCE (Fig. 2(B) curve (c)), it shows higher magnitude

current for GO*x*, FAD redox couples and Au oxidation process. Hence, these results illustrate that for this type of nano biocomposite film process, the GCE is more active than the other electrodes. Furthermore the active surface coverage concentrations (Γ) of the nano biocomposite film were compared with three different types of electrodes (GCE, GE and SPCE) and given in Table I.[35–37] From the active surface coverage concentration values of these electrodes, we can notice that GCE shows the enhanced Γ value for *f*-MWCNTs-Au-GO*x* nano biocomposite film. According to these results, it was ascertained that GCE has the good compatibility for this type of nano biocomposite films.

Next the *f*-MWCNTs-Au-GO*x* biocomposite film has been examined in various pH buffer solutions (figure not shown). In various pH solutions (5 to 13), it was found that the nano biocomposite film is highly stable with three redox peak currents, respectively. Perhaps, the film involves an ion exchange; our suggestion is that the reduction currents of the nano biocomposite film include a proton transfer. Here the Ep_a and Ep_c values of the nano biocomposite film depend on the pH value of the buffer solution. Furthermore, the formal potentials of *f*-MWCNTs-Au-GO*x* biocomposite film plotted over a pH range of 5 to 13. From this plot, the slope value was found as −50 mV/pH, which suggests that the overall reaction of the film comprises equal number of electrons and protons transfer process.[38]

3.2. Topographic Characterization of *f*-MWCNTs-Au-GO*x* Using SEM, and AFM

The Au-GO*x*, *f*-MWCNTs-GO*x* and *f*-MWCNTs-Au-GO*x* biocomposite films have been prepared on indium tin oxide (ITO) with similar conditions and similar potential as that of GCE and characterized by using SEM and AFM techniques. The 60° angle SEM view of Au-GO*x* (Fig. 3(A)) on the ITO electrode shows that nano Au has formed as round shaped and homogeneously dispersed and adhered on the ITO surface. The *f*-MWCNTs-GO*x* on the ITO electrode (Fig. 3(B)) shows *f*-MWCNTs with uniform layered structural formation of GO*x*. Figures 3(C and D) are the top and 60° angle SEM views of *f*-MWCNTs-Au-GO*x* film on the ITO electrode

Table I. Active surface coverage concentrations (Γ) of Au, GO*x* and FAD at different type electrodes using CV in 0.1 mol L⁻¹ PBS (pH 7.4).

| Type of electrode	Type of film	Γ of Au (mol cm⁻²)	Γ of GO*x* (mol cm⁻²)	Γ of FAD (mol cm⁻²)
GCE	Au-GO*x*	8.47×10^{-11}	—	1.89×10^{-11}
	f-MWCNTs-GO*x*	—	1.15×10^{-10}	7.01×10^{-11}
	f-MWCNTs-Au	1.02×10^{-9}	—	—
	f-MWCNTs-Au-GO*x*	4.86×10^{-10}	2.05×10^{-10}	1.74×10^{-10}
Gold	*f*-MWCNTs-Au-GO*x*	1.32×10^{-9}	6.73×10^{-11}	1.64×10^{-10}
SPCE[a]	*f*-MWCNTs-Au-GO*x*	4.26×10^{-10}	2.01×10^{-11}	5.59×10^{-11}

[a]Screen printed carbon electrode (SPCE).
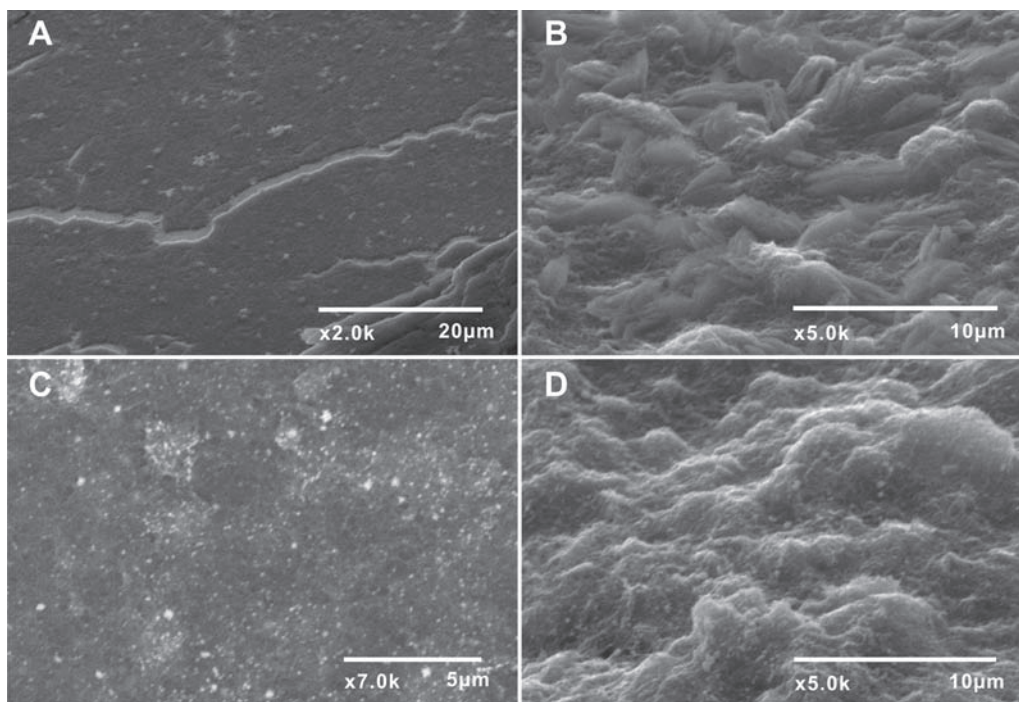
Fig. 3. SEM images of (A) Au-GO*x*, (B) *f*-MWCNTs-GO*x* (C) and (D) are top and 60° views of *f*-MWCNTs-Au-GO*x* biocomposite enzyme film.

which show an obvious formation of nano biocomposite film. From these SEM analysis results it was found that the particle size distribution of Au varies from 50–80 nm, respectively.

The AFM tapping mode operation is particularly useful for imaging soft sample surfaces, such as biological specimens. Figures 4(A), (B) and (C) depicts the surface topographic images of Au-GO*x*, *f*-MWCNTs-GO*x* and *f*-MWCNTs-Au-GO*x* films using AFM. In Figures 4(A) and (C) the numerous globular particle structure formations show the presence of Au in Au-GO*x* and *f*-MWCNTs-Au-GO*x* films. However, in Figure 4(B) there is no particular structure noticed and it is an *f*-MWCNTs-GO*x* film. Further the *f*-MWCNTs-Au-GO*x* biocomposite film shows big globular structure, it is the huge accumulation of *f*-MWCNTs and GO*x* on the ITO electrode; the smaller particular structure is nano Au. Above these results, and comparing all the (A), (B) and (C) SEM images, *f*-MWCNTs-Au-GO*x* film looks like an obvious structure in AFM analysis. Further based on the previous literature reports, it was found that the electrodes with higher roughness values will have the good catalytic activity.[39, 40] From the AFM results of *f*-MWCNTs-Au-GO*x* (26 nm) composite film, it was found that it have the high roughness average (26 nm) value comparing with Au-GO*x* (16.2 nm) and *f*-MWCNTs-GO*x* (20.8 nm) films, respectively. This shows that the *f*-MWCNTs-Au-GO*x* film have good electro catalytic activity rather than Au-GO*x* and *f*-MWCNTs-GO*x* films. Finally, the comparison results of these films in SEM and AFM methods corroborates well.

3.3. Electrochemical Imaging of *f*-MWCNTs-Au-GO*x* by SECM

The SECM experiments for *f*-MWCNTs-Au-GO*x* imaging have been carried out using 7 μm platinum ultra microelectrode (UME) in 0.1 M KCl aqueous solution containing 1×10^{-3} mol L^{-1} potassium hexacyanoferrate (III) as redox mediator and the tip potential and substrate (composite film) potential has been held at 0 V and 0.5 V, respectively (vs. Ag/AgCl). This technique is a scanning probe technique which is based on faradic current changes as the UME tip moves across the sample surface. The SECM image was based on the parameters such like sample topography and surface reactivity, so this technique could be used to examine differences in electrochemical activity of surfaces at high resolution.[41] Figures 5(A) and (B) shows the SECM image and the cross sectional view of the *f*-MWCNTs-Au-GO*x* film current, scanned over 100 μm $\times$ 100 μm region using UME in close proximity to the modified GCE surface. Further the three dimensional views (Fig. 5(C)) shows the high current regions of the *f*-MWCNTs-Au-GO*x* biocomposite film. Here the pink color regions arisen in Figure 5(A) represents higher UME tip current at *f*-MWCNTs-Au-GO*x* film, indicates the high current (thickness) area of the film, and the remaining green colored area depicts the whole film area. Further the red color region indicates the low feedback current of the composite film. Furthermore, the reaction mechanism for this type of topographic imaging could be explained by the redox property of potassium
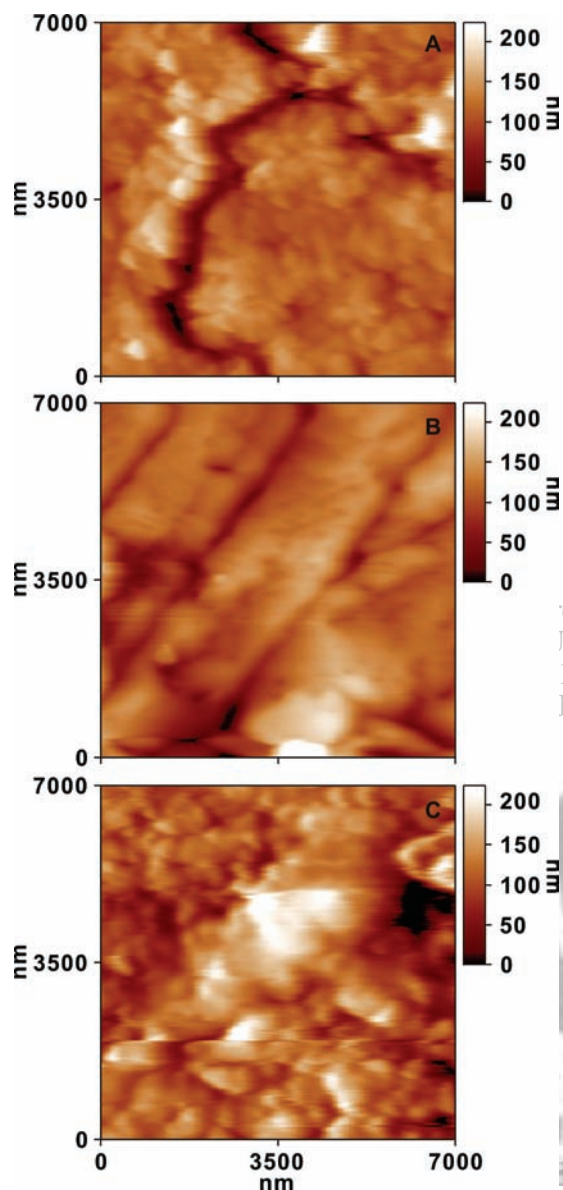
Fig. 4. AFM images of (A) Au-GO*x*, (B) *f*-MWCNTs-GO*x* and (C) *f*-MWCNTs-Au-GO*x* biocomposite enzyme film.

hexacyanoferrate (III); while the tip approaches towards the conductive substrate, leading to the positive feedback current at the UME tip. Similar type of results has been reported for NF with CNT composite samples.[42]

3.4. Electroanalytical Response and Amperometric Sensing Application of *f*-MWCNTs-Au-GO*x* for LC Detection

The proposed *f*-MWCNTs-Au-GO*x* film modified GCE has been successfully employed for the detection of LC. Before employing the *f*-MWCNTs-Au-GO*x* film, the comparison study has been done for the LC detection using other films (*f*-MWCNTs-GO*x* and Au-GO*x* modified GCE). Here Figure 6 shows the electrocatalytic
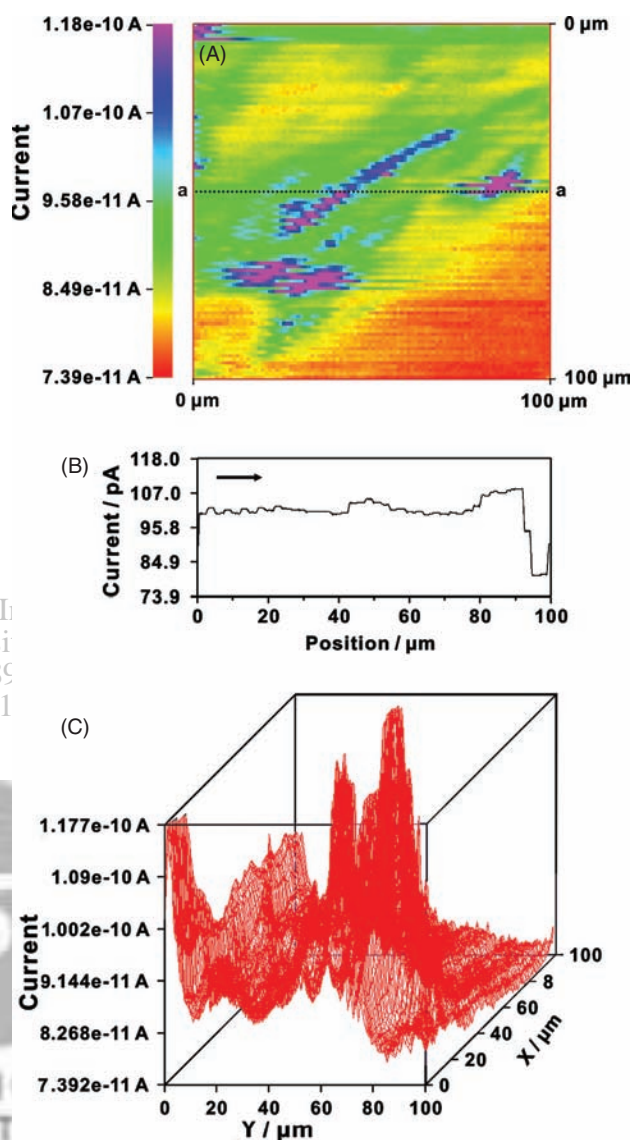
Fig. 5. (A) SECM image of the surface of *f*-MWCNTs-Au-GO*x* nano biocomposite film modified GCE using 7 μm Pt UME tip in 0.1 mol L^{-1} KCl containing 1×10^{-3} mol L^{-1} K$_3$Fe(CN)$_6$ as redox mediator. (B) Cross-sectional view of current along "a–a" in dashed line. (C) 3D view of the *f*-MWCNTs-Au-GO*x* biocomposite enzyme film modified GCE.

oxidation of LC (2×10^{-4} mol L^{-1} in pH 7.4 PBS) on the various types of film modified GCE. The LC electro oxidation, at bare GCE (curve a$'$) takes place at 0.8 V (electro catalytic oxidation peak current for LC = 1.39 μA), at the same time, for Au-GO*x*, (curve b) and *f*-MWCNTs-GO*x* (curve a) film modified GCEs the detection of LC exhibits at 0.77 and 0.76 V with much enhanced electro oxidation peak currents (19 and 7.6 μA). On the other hand, for *f*-MWCNTs-Au-GO*x* film modified GCE (curve c), it shows much enhanced electro oxidation peak for the LC detection at 0.75 V (current (25.8 μA)) comparing with *f*-MWCNT-GO*x* and Au-GO*x* film modified GCEs,
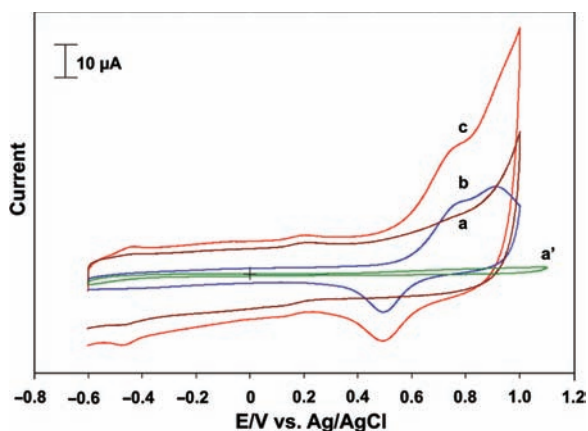
Fig. 6. (A) CVs of the (a) f-MWCNTs-GOx (b) Au-GOx (c) f-MWCNTs-Au-GOx modified GCE and (a′) bare GCE in pH 7.4 PBS containing LC = 2×10^{-4} mol L^{-1}.

respectively. Therefore, based on this context, we came to decision that the f-MWCNT-Au-GOx film possesses the good electro catalytic activity for LC detection comparing with the other film modified GC electrodes. Thus, here we have employed the f-MWCNT-Au-GOx film modified GCE for the detailed studies of LC detection using CV and amperometric studies, respectively.

Figure 7(A) shows the CVs of the electrochemical oxidation of L-cysteine (LC) on f-MWCNTs-Au-GOx biocomposite film and bare GCE for various concentrations of LC in pH 7.4 PBS. Here the oxidation peak of LC has been appeared on f-MWCNTs-Au-GOx biocomposite film at $Ep_a = 0.75$ V. Further for increasing concentrations (curves a–d) of LC the oxidation peak currents of f-MWCNTs-Au-GOx biocomposite film increases linearly with good stability. While comparing with f-MWCNTs-Au-GOx biocomposite film, bare GCE (a′) shows poor oxidation current response for the LC oxidation. The inset in Figure 7(A) shows the current versus concentration plot of LC on f-MWCNTs-Au-GOx biocomposite enzyme film modified GCE. Further the Figure 7(B) shows the amperometric response of the f-MWCNTs-Au-GOx film for the successive additions of LC in the higher concentration range from 0.1 to 1.08×10^{-3} mol L^{-1} (at 0.75 V), respectively. In these results too, the amperometric current response of LC oxidation reached within 5 seconds following the additions of LC and the current response were directly proportional to the concentrations. Further from the calibration plot, the slope value for the LC oxidation has been found as 553.3 μA L mmol^{-1} (Fig. 7(B) inset (d)) with a correlation coefficient of 0.9924. Also, the sensitivity ($n = 9$) for the LC oxidation has been found as 312.60 μA L mmol^{-1}cm^{-2}, respectively. Next the in the Figure 7(B) inset (C) shows the low concentration range detection of LC in the linear range of 2 to 42×10^{-6} mol L^{-1}, with a slope value
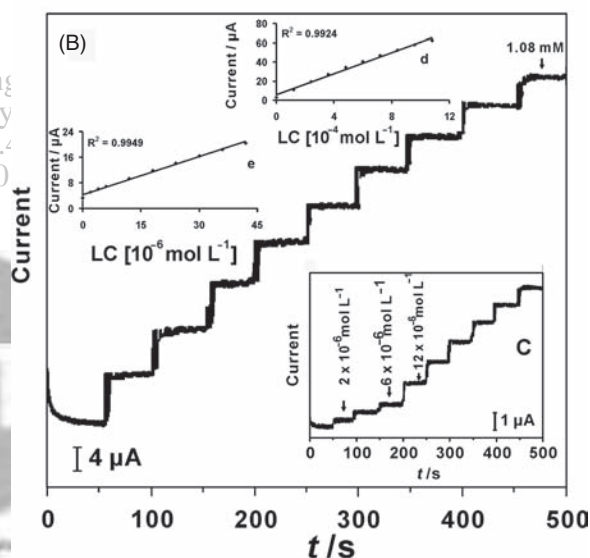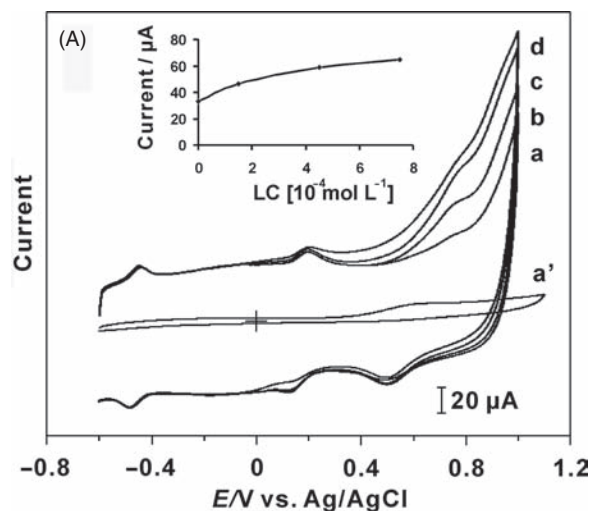
Fig. 7. (A) CVs of the f-MWCNTs-Au-GOx biocomposite enzyme film in pH 7.4 PBS with various concentration of LC: (a′) bare GC with [LC] = 7.5×10^{-4} mol L^{-1}, [LC] = (a) 0.0, (b) 1.5 (c) 4.5 and (d) 7.5×10^{-4} mol L^{-1}. The inset in (A) shows the plot of current versus different concentration of LC for f-MWCNTs-Au-GOx composite film. (B) Amperometric i–t curve of the f-MWCNTs-Au-GOx composite film in pH 7.4 PBS from 0.12 to 1.08×10^{-3} mol L^{-1} and (C) from 2 to 42×10^{-6} mol L^{-1} of LC at 0.75 V. The insets in (B) were the calibration curve for LC, where (d) high and (e) low concentrations of LC.

(Fig. 7(B) inset (e)) of 0.396 μA L mmol^{-1}, the correlation coefficient = 0.9949. Furthermore, the sensitivity ($n = 9$) for LC oxidation in low concentration range was found as 0.22 μA L mmol^{-1}cm^{-2}, respectively. Above these results validates that the f-MWCNTs-Au-GOx modified GCE is capable for the electro catalytic oxidation of LC in lower and higher concentration ranges. Also, the proposed film possesses the linear range of detection for the LC electro oxidation using CV and amperometry which has been compared with previous literature reports and the details were listed in the Table II.
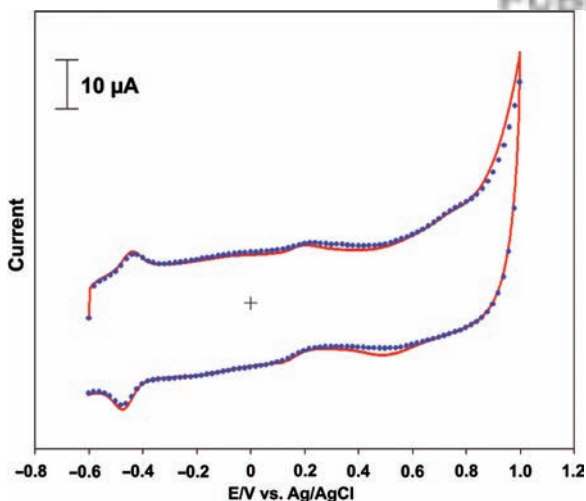
Table II. Comparison table for various LC sensors.

Electrode	Analytical range (mol L^{-1})	pH	Ref.
Cytochrome C and DNA/GCE	$8.0 \times 10^{-4} - 4.0 \times 10^{-3}$ [a]	8.3	[10]
Zinc phthalocyanine complexes/GCE	$1.5 \times 10^{-6} - 1.0 \times 10^{-3}$ [a]	4.0	[11]
Ruthenium oxide/hexacyanoferrate/GCE	$1.0 \times 10^{-3} - 2.0 \times 10^{-3}$ [a]	1.5	[12]
Poly(nickel tetrakis(*N*-methyl-4-pyridyl)porphyrin) tetratosylate/GCE	$7.0 \times 10^{-3} - 2.1 \times 10^{-2}$ [a]	13	[14]
Rutheniumoxide/hexacyanoferrate/silicomolybdate hybrid films/GCE	$2.0 \times 10^{-4} - 8.0 \times 10^{-4}$ [a]	1.5	[15]
Functionalized multi-wall carbon nanotubes/GCE	$3.0 \times 10^{-7} - 8.0 \times 10^{-3}$ [c]	3.0	[17]
Ferrocenecarboxylic acid modified carbon paste electrode	$1.0 \times 10^{-5} - 1.0 \times 10^{-3}$ [a] $4.1 \times 10^{-8} - 3.7 \times 10^{-5}$ [b]	7.0	[19]
Ferrocene dicarboxylic acid modified carbon paste electrode	$3.0 \times 10^{-5} - 2.2 \times 10^{-3}$ [a] $1.5 \times 10^{-5} - 3.2 \times 10^{-3}$ [b]	8.0	[21]
Carbon ionic liquid electrode	$2.0 \times 10^{-6} - 2.0 \times 10^{-4}$ [a]	7.0	[22]
Erbium hexacyanoferrate-modified carbon ceramic electrode	$5.0 \times 10^{-6} - 1.3 \times 10^{-4}$ [c]	7.0	[23]
Polyoxometalate modifiedcarbon paste electrode	$5.0 \times 10^{-3} - 3.0 \times 10^{-2}$ [a]	3.8	[24]
f-MWCNTs-Au-GO*x*/GCE	$1.5 \times 10^{-4} - 7.5 \times 10^{-4}$ [a] $2.0 \times 10^{-6} - 1.08 \times 10^{-3}$ [c]	7.4	This work

[a]Cyclic voltammetry, [b]Differential pulse voltammetry, [c]Amperometry.

3.5. Repeatability and Stability of the *f*-MWCNTs-Au-GO*x* Modified Electrode

The *f*-MWCNTs-Au-GO*x* film modified GCE presented good repeatability for LC determination. The relative standard deviation (% RSD) of the peak current for ten determinations of 7.5×10^{-4} mol L^{-1} LC was found as 3.1%. Further the stability nature of the proposed film has been examined using CV. Here, Figure 8 displays the CVs of the *f*-MWCNTs-Au-GO*x* film in 0.1 mol L^{-1} PBS (pH 7.4). The red colored solid curve in Figure 8 shows the initially scanned CV of the *f*-MWCNTs-Au-GO*x* film modified GCE. After this process, the *f*-MWCNTs-Au-GO*x* film modified GCE has been stored in 0.1 mol L^{-1} PBS (pH 7.4) at 4 °C for four days. After four days, the same film modified GCE was scanned again in pH 7.4 PBS solutions and corresponding CV response has been shown as

blue colored dotted line in the Figure 8. Here, by comparing both the solid and dotted CVs, we can conclude that the *f*-MWCNTs-Au-GO*x* film modified GCE almost 95% stable for four days at 4 °C. At the same time, only a small current decrease observed for Au reduction at around 0.50 V. Finally, this examination result clearly validates the stability nature of the *f*-MWCNTs-Au-GO*x* film modified GCE, respectively.

4. CONCLUSION

In this study, we have developed a nano biocomposite film by using the functionalized MWCNTs incorporated with nano Au and GO*x* at GCE and ITO electrode surface. The presence of *f*-MWCNTs and nano Au enhances the electrocatalytic property and current magnitude of film. The proposed nano biocomposite film possesses the advantages of easy fabrication, high reproducibility and sufficient long-term stability. Also, the proposed nano biocomposite film shows a good sensitivity for the rapid detection of LC with good repeatability and stability. Therefore, this work establishes and illustrates, in principle and potential, a simple and novel approach for the development of LC amperometric sensor based on *f*-MWCNTs-Au-GO*x* composite film.

References and Notes

1. I. M. Kolthoff and C. Barnum, *J. Am. Chem. Soc.* 62, 3061 (**1940**).
2. F. G. Banina, J. C. Moreira, and A. G. Fogg, *The Analyst* 119, 309 (**1994**).
3. D. G. Davis and E. Bianco, *J. Electroanal. Chem.* 12, 254 (**1966**).
4. J. Koryta and J. Prodac, *J. Electroanal. Chem.* 17, 185 (**1968**).
5. J. A. Reynaud, B. Maltoy, and P. Canessau, *J. Electroanal. Chem.* 114, 195 (**1980**).

Fig. 8. CVs of the *f*-MWCNTs-Au-GO*x* composite enzyme film at the initial scanning (red colored solid curve) and after four days (blue colored dotted curve) in pH 7.4 PBS.

6. M .E. Johll, D. G. Williams, and D. C. Johnson, *Electroanalysis* 9, 1397 (**1997**).

7. S.-M. Chen, *Electrochim Acta* 42, 1663 (**1997**).

8. C. Sun, S. Qin and Y. Luo, *Electroanalysis* 11, 1236 (**1999**).

9. W. T. Tan, A. M. Bond, S. W. Ngooi, E. B. Lim, and J. K. Goh, *Anal. Chim. Acta* 491, 181 (**2003**).

10. S.-M. Chen and S.-V. Chen, *Electrochim Acta* 48, 513 (**2003**).

11. J. Obirai and T. Nyokong, *Electrochim Acta* 50, 5427 (**2005**).

12. S.-M. Chen, M.-F. Lu, and K.-C. Lin, *J. Electroanal. Chem.* 579, 163 (**2005**).

13. B. Keita, R. Contant, P. Mialane, F. Sécheresse, P. Oliveira, and L. Nadjo, *Electrochem Commun.* 8, 767 (**2006**).

14. S.-M. Chen and C.-H. Wang, *J. Solid State Electrochem.* 11, 581 (**2007**).

15. S.-M. Chen and J.-L. Song, *J. Electroanal. Chem.* 599, 41 (**2007**).

16. S. Griveau, M. Gulppi, J. Pavez, J. Zagal, and F. Bedioui, *Electroanalysis* 15, 779 (**2003**).

17. X.-N. Cao, L. Lin, Y.-Z. Xian, W. Zhang, Y.-F. Xie, and L.-T. Jin, *Electroanalysis* 15, 892 (**2003**).

18. D. Mimica, F. Bedioui, and J. Zagal, *Electrochim Acta* 48, 323 (**2002**).

19. J.-B. Raoof, R. Ojani, and M. Kolbadinezhad, *Electroanalysis* 17, 2043 (**2005**).

20. K. I. Ozoemena and T. Nyokong, *Electrochim Acta* 51, 2669 (**2006**).

21. J.-B. Raoof, R. Ojani, and H. Beitollahi, *Electroanalysis* 19, 1822 (**2007**).

22. N. Maleki, A. Safavi, F. Sedaghati, and F. Tajabadi, *Anal Biochem.* 369, 149 (**2007**).

23. Q.-L. Sheng, H. Yu, and J.-B. Zheng, *J. Solid State Electrochem.* 12, 1077 (**2008**).

24. C. Li, R. Cao, K. O' Halloran, H. Ma, and L. Wu, *Electrochim Acta* 54, 484 (**2008**).

25. C. Lei and J. Deng, *Anal. Chem.* 68, 3344 (**1996**).

26. Y. Zhou, N. Hu, Y. Zeng, and J. F. Rusling, *Langmuir* 18, 211 (**2002**).

27. Z. Dai, H. X. Ju, and H. Y. Chen, *Electroanalysis* 17, 862 (**2005**).

28. B. Liu, F. Tan, J. Kong, and J. Deng, *Anal. Chim. Acta* 386, 31 (**1999**).

29. I. Willner, V. H. Shabtai, R. Blonder, E. Katz, G. Tao, A. F. Buckmann, and A. Heller, *J. Am. Chem. Soc.* 118, 10321 (**1996**).

30. E. Katz, V. H. Shabtai, A. Bardea, I. Willner, H. K. Rau, and W. Haehnel, *Biosens. Bioelectron.* 13, 741 (**1998**).

31. Y. Xiao, F. Patolsky, E. Katz, J. F. Hainfeld, and I. Willner, *Science* 299, 1877 (**2003**).

32. K. Yamashita, M. Takagi, K. Uchida, H. Kondo, and S. Takenaka, *Analyst* 126, 1210 (**2001**).

33. J. Wang, F. Song, and F. Zhou, *Langmuir* 18, 6653 (**2002**).

34. Y. Yan, M. Zhang, K. Gong, L. Su, Z. Gu, and L. Mao, *Chem. Mater.* 17, 3457 (**2005**).

35. Y. Li and G. Shi, *J. Phy. Chem. B* 109, 23787 (**2005**).

36. A. I. Gopalan, K. P. Lee, K. M. Manesh, P. Santhosh, and J. H. Kim, *J. Mol. Catal. A Chem.* 256, 335 (**2006**).

37. U. Yogeswaran, S. Thiagarajan, and S.-M. Chen, *Carbon* 45, 2783 (**2007**).

38. P. Monk, Fundamentals of Electroanalytical Chemistry, John Wiley & Sons Ltd, England (**2001**).

39. F. Marken, S. Kumbhat, G. H. W. Sanders, and R. G. Compton, *J. Electroanal. Chem.* 414, 95 (**1996**).

40. L. Fojt and S. Hasoò, *J. Electroanal. Chem.* 586, 136 (**2006**).

41. D. O. Wipf and A. J. Bard, *J. Electrochem. Soc.* 138, 469 (**1991**).

42. H. S. Wang, T. H. Li, W. L. Jia, and H. Y. Xu, *Biosens and Bioelectron.* 22, 664 (**2006**).